Supplementary Material

Microbial communities in the East and West Fram Strait during sea-ice melting season

Eduard Fadeev[1,2], Ian Salter[1,3], Vibe Schourup-Kristensen[1], Eva-Maria Nöthig[1], Katja Metfies[1,4], Anja Engel[5], Judith Piontek[5], Antje Boetius[1,2], Christina Bienhold*[1,2]

[1] Alfred Wegener Institute, Helmholtz Center for Polar and Marine Research, Bremerhaven, Germany

[2] Max Planck Institute for Marine Microbiology, Bremen, Germany

[3] Faroe Marine Research Institute, Torshavn, Faroe Islands

[4] Helmholtz Institute for Functional Marine Biodiversity, Oldenburg, Germany

[5] GEOMAR Helmholtz Centre for Ocean Research, Kiel, Germany

*__Correspondence__: Christina Bienhold - Christina.Bienhold@awi.de

Keywords: Arctic Ocean, phytoplankton bloom, microbial interactions, bacterioplankton, network analysis

1 Tables and figures

Supplementary Table 1: Overview of sampled stations during RV Polarstern expedition PS85. The table consists of sampling information for each station, number of sequences in each step of the bioinformatics workflow as well as alpha diversity estimations, conducted using the R package 'iNEXT'.

PANGAEA stationID*	Station Name	Longitude [°east]	Latitude [°north]	Sampling Date [dd-mm-yyyy]	Depth [m]	Community fraction	No. of raw amplicons	No. of amplicons after QC and merging	Final no. of amplicons after taxonomic assignment	Observed richness (no. of OTUs)	Chao richness estimator	Richness coverage (%)	Shanon diversity index	Sample completeness
PS85/0426-1	10W	-9.93	78.81	16-06-2014	5	BAC-PA	80397	64742	33796	1253	1688.989	74%	96.35	98.71
						EUK	147259	96416	79400	1375	1626.604	85%	101.524	99.53
					25	BAC-PA	91123	72119	52012	1517	2195.084	69%	50.779	98.84
						EUK	150194	102204	72574	1061	1227.225	86%	59.651	99.66
					40	BAC-PA	32709	14861	10612	664	833.085	80%	109.306	98.19
						EUK	147314	100351	63842	964	1053.573	91%	83.285	99.73
PS85/0485-1	1E	1.01	78.84	28-06-2014	5	BAC-FL	36556	15425	12513	442	1048.766	42%	32.742	97.95
						BAC-PA	52802	26634	24811	649	1309.439	50%	30.321	98.63
						EUK	62815	42857	25060	549	894.012	61%	28.08	99.07
					15	BAC-FL	76337	36003	29384	860	1767.938	49%	38.251	98.35
						BAC-PA	41723	20613	17462	498	931.475	53%	30.32	98.54
						EUK	121572	78223	25238	548	866.662	63%	23.145	99.09
					60	BAC-FL	43652	20877	19360	640	1497.575	43%	77.441	98.25
						BAC-PA	35591	17538	16430	438	966.968	45%	26.964	98.6
						EUK	169597	109653	81993	1258	1766.633	71%	76.014	99.42
PS85/0482-1	1W	-0.9	78.83	28-06-2014	5	BAC-FL	77709	61309	46317	1858	3356.522	55%	61.454	97.86
						BAC-PA	90364	71325	52816	1847	3229.015	57%	61.226	98.17
						EUK	99943	62021	40492	605	925.078	65%	22.675	99.4
					30	BAC-FL	60089	48421	41956	1982	3679.578	54%	87.374	97.44
						BAC-PA	75761	61646	50193	1732	3330.309	52%	52.392	98.13

Supplementary Material

						EUK	116173	73992	28927	647	981.392	66%	25.073	99.07
					50	**BAC-FL**	76494	61438	55904	2591	4581.841	57%	103.816	97.55
						BAC-PA	84659	66948	55419	1912	3219.017	59%	48.069	98.32
						EUK	164612	108612	62359	1188	1662.177	71%	56.479	99.29
PS85/0432-1	**7W**	**-7.01**	**78.66**	**17-06-2014**	**5**	**BAC-FL**	70906	57234	44915	1911	3496.327	55%	122.414	97.75
						BAC-PA	78260	62880	29441	1574	2363.784	67%	155.048	97.9
						EUK	33567	7152	4598	348	381.969	91%	88.583	98.35
					15	**BAC-FL**	82651	65466	53898	2031	3823.79	53%	142.557	98.04
						BAC-PA	89928	70465	36222	1560	2122.192	74%	116.708	98.42
						EUK	104233	69591	22287	309	419.033	74%	17.881	99.52
					30	**BAC-FL**	89980	71294	62394	2636	4061.895	65%	202.823	98.07
						BAC-PA	91899	72800	47748	1699	2274.69	75%	80.466	98.73
						EUK	125204	80222	68398	539	587.905	92%	23.078	99.89
PS85/0429-1	**8.5W**	**-8.56**	**78.83**	**16-06-2014**	**5**	**BAC-FL**	41349	20557	18329	863	1958.207	44%	70.145	97.41
						BAC-PA	91168	79425	45569	1081	1365.313	79%	52.884	99.32
						EUK	122102	82354	66153	1362	1634.753	83%	110.443	99.47
					15	**BAC-FL**	41747	19198	16582	760	1316.677	58%	79.439	97.97
						EUK	181419	119906	96066	1850	1994.488	93%	185.048	99.65
					30	**BAC-FL**	32931	14862	13682	763	1139.896	67%	147.079	97.95
						BAC-PA	29010	13160	9141	733	984.988	74%	120.82	97.22
						EUK	129949	87319	63611	1280	1415.733	90%	186.098	99.67
PS85/0437-1	**EG1**	**-5.5**	**78.83**	**17-06-2014**	**5**	**BAC-FL**	85231	68633	57782	2314	3836.833	60%	85.837	98
						BAC-PA	78359	62571	29282	1349	2218.654	61%	79.971	97.88
						EUK	196875	131887	93201	1028	1308.414	79%	44.659	99.65
					25	**BAC-FL**	81707	66199	56587	2672	4327.635	62%	107.536	97.65
						BAC-PA	85414	70034	20038	995	1623.54	61%	55.01	97.8
						EUK	110323	72002	26192	775	1006.473	77%	56.593	99.05
					30	**BAC-FL**	95756	76869	65384	2501	4799.385	52%	145.749	97.93
						BAC-PA	81069	65846	25796	1225	1761.604	70%	107.519	98.15
						EUK	71733	49058	30306	721	911.254	79%	45.824	99.3
PS85/0444-1	**EG3**	**-3.98**	**78.84**	**18-06-2014**	**5**	**BAC-FL**	77088	61503	50149	2009	3734.522	54%	127.557	97.93
						BAC-PA	61815	49003	20694	1254	1973.635	64%	114.642	97.54

						EUK	140298	96787	81029	837	920.111	91%	31.81	99.82
					25	**BAC-FL**	78705	61132	54206	2286	3890.246	59%	173.945	98.07
						BAC-PA	72914	56244	39354	1731	2271.522	76%	82.698	98.43
						EUK	69062	25775	16066	707	974.455	73%	108.43	98.52
					30	**BAC-FL**	86092	68494	59783	2394	4015.66	60%	192.309	98.13
						BAC-PA	103314	79525	50683	1581	2034.906	78%	68.442	98.97
						EUK	111864	77280	57390	1059	1120.875	94%	106.914	99.74
PS85/0455-2	**EG4**	**-2.83**	**78.45**	**21-06-2014**	**5**	**BAC-FL**	76892	62268	47336	2276	4224.997	54%	92.664	97.37
						BAC-PA	75665	58788	32510	1478	2712.614	54%	58.3	97.65
						EUK	124988	82632	62200	1044	1571.87	66%	38.549	99.34
					20	**BAC-FL**	81102	64823	52158	2088	3396.112	61%	127.548	98.06
						BAC-PA	82155	66160	41640	1311	1849.317	71%	44.527	98.74
						EUK	138829	90341	69354	866	1029.682	84%	24.146	99.67
					30	**BAC-FL**	78368	61711	51762	2610	4652.97	56%	160.179	97.36
						BAC-PA	97030	74544	51986	1460	2038.56	72%	66.581	98.96
						EUK	124644	83373	68622	1076	1396.831	77%	31.301	99.49
PS85/0470-1	**HG1**	**6.08**	**79.13**	**24-06-2014**	**5**	**BAC-PA**	88309	69223	61358	1288	1858.022	69%	23.269	99.13
						EUK	118376	81039	63494	660	844.886	78%	34.948	99.67
					23	**BAC-FL**	44197	22004	20405	713	1586.577	45%	52.653	97.95
						BAC-PA	99612	76756	53722	1221	1806.67	68%	33.33	99.02
						EUK	114736	73485	52638	618	939.635	66%	45.408	99.57
					30	**BAC-FL**	47998	23509	21405	956	2383.473	40%	80.572	97.35
						BAC-PA	94944	74271	45745	1244	1997.736	62%	40.518	98.68
						EUK	106104	70476	28501	758	1097.497	69%	78.057	99.03
PS85/0460-1	**HG4**	**4.19**	**79.19**	**22-06-2014**	**5**	**BAC-FL**	58239	28496	24334	947	2171.471	44%	58.602	97.81
						BAC-PA	77468	62783	49002	1062	1824.041	58%	24.182	98.92
						EUK	24794	17367	14697	406	580.37	70%	49.206	98.95
					50	**BAC-FL**	51128	23529	20639	799	1725.055	46%	55.445	97.86
						BAC-PA	80709	64555	55532	1614	2817.068	57%	44.455	98.54
						EUK	122028	83737	63358	920	1477.246	62%	28.191	99.37
					60	**EUK**	127462	86970	65048	1079	1457.086	74%	39.692	99.41
PS85/0465-1	**HG9**	**2.75**	**79.15**	**24-06-2014**	**5**	**BAC-FL**	47806	23211	20885	669	1424.969	47%	40.364	98.19

Supplementary Material

						BAC-PA	40295	20267	18718	565	1206.308	47%	28.328	98.37
					20	**BAC-FL**	83762	40055	35179	1762	3372.888	52%	88.644	97.15
					50	**BAC-FL**	74227	35523	31476	1343	2580.334	52%	110.919	97.78
PS85/0473-1	**N4**	**4.26**	**79.76**	**25-06-2014**	**5**	**BAC-FL**	78003	61567	51392	1820	2985.597	61%	46.664	98.23
						BAC-PA	80864	64261	50661	1696	2866.384	59%	50.195	98.35
						EUK	104829	66993	46176	743	1159.061	64%	45.615	99.33
					40	**BAC-FL**	76360	59989	54801	2386	4029.084	59%	90.256	97.79
						BAC-PA	79049	62868	53831	1500	2607.397	58%	37.941	98.57
						EUK	1375615	932321	668065	2706	2969.087	91%	14.449	99.92
					55	**BAC-FL**	87573	69600	63000	2583	4378.365	59%	103.08	97.96
						BAC-PA	73018	57336	48538	1390	2243.044	62%	34.07	98.65
						EUK	184908	127835	100293	1163	1673.722	69%	39.768	99.58

*PANGAEA - www.pangaea.de

Supplementary Table 2: Bacterial cell abundance and activity in East Greenland Current (EGC) and West Spitsbergen Current (WSC). The values represent the mean and the standard deviation for each parameter and the number in parentheses represents the number of samples.

	EGC	**WSC**
Total bacterial cell conc. [cells ml^{-1}]	5.1 ± 0.2 (11)	5.8 ± 0.1 (12)
HNA/LNA cells ratio*	1.8 ± 0.6 (11)	3.1 ± 1.2 (12)
Total bacterial productivity [pmol leucine $Liter^{-1}$ $hour^{-1}$]	6.3 (18)	25.4 (17)
Cell specific bac. prod. [10e-8 pmol leucine $cell^{-1}$ $hour^{-1}$]	3.3 ± 2.4 (11)	3.7 ± 3.2 (12)

*HNA - high nucleic acids, LNA- low nucleic acids.

Supplementary Material

Supplementary Table 3: Properties of the co-occurrence networks in both Free-living (FL) and particle-attached (PA) size fractions.

	FL network	**PA network**
Nodes		
No. of nodes	555	514
Bacterial nodes (% of total)	55 (74%)	85 (64%)
Edges		
No. of edges	718	986
Pos. edges (% of total)	607 (85%)	702 (71%)
Topology		
No. clusters	49	52
Modularity	0.39	0.27
Diameter	23.09	15.68
Mean degree	2.58	3.83
Avg. path length	8.56	4.78
Betweenness	497.24	681.51

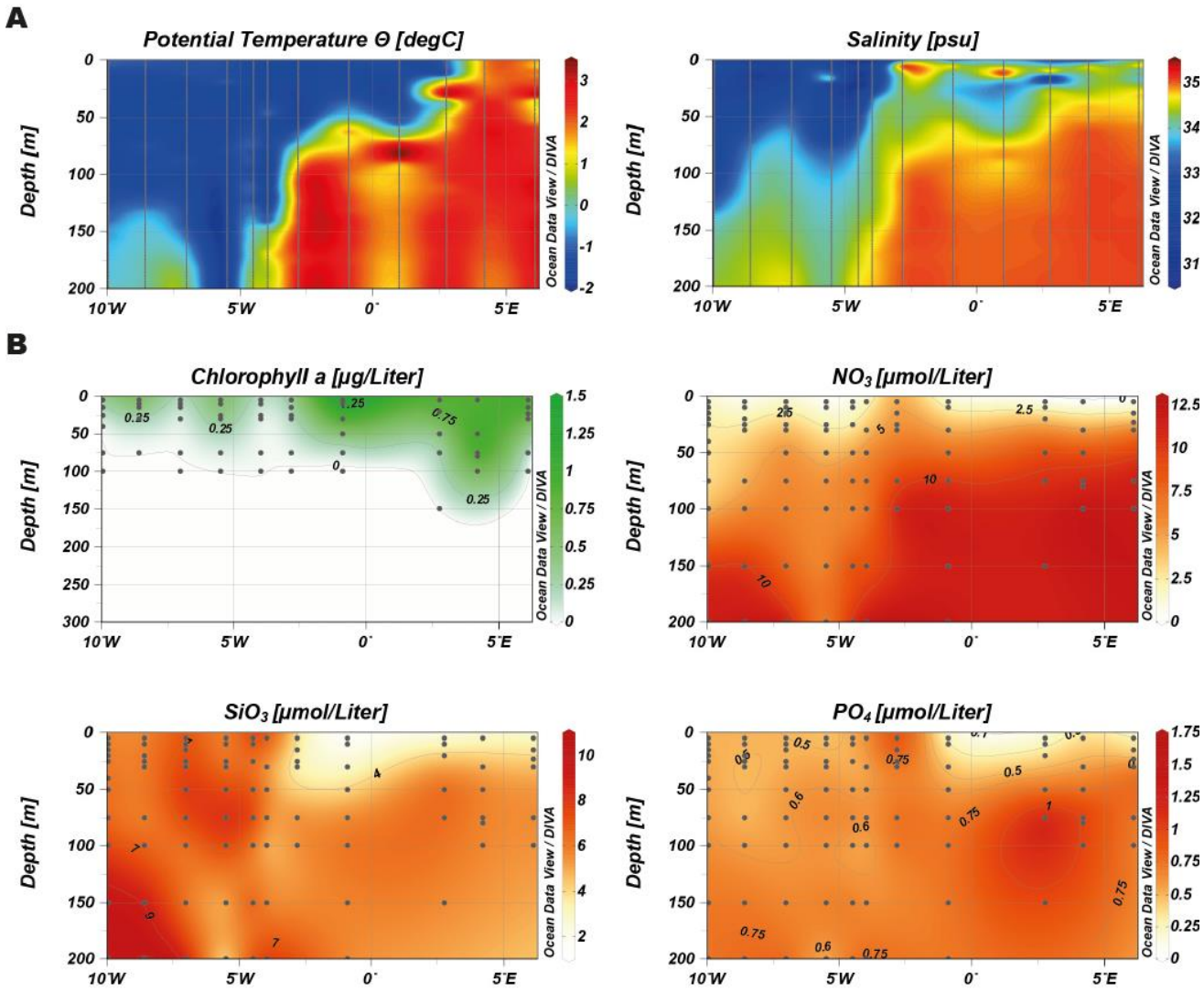

Supplementary Figure 1: Regional separation of Fram Strait based on in situ biogeochemical parameters. (**A**) Physical characteristics of the water column from CTD (Conductivity-Temperature-Depth) sensors. (**B**) Chl a and inorganic nutrients measured in situ. The longitudinal coordinates of EGC region are 10W-1W, and 1W-6E for the WSC region. The plot was generated using Ocean Data View (v4.7.10; Schlitzer, 2015).

Supplementary Material

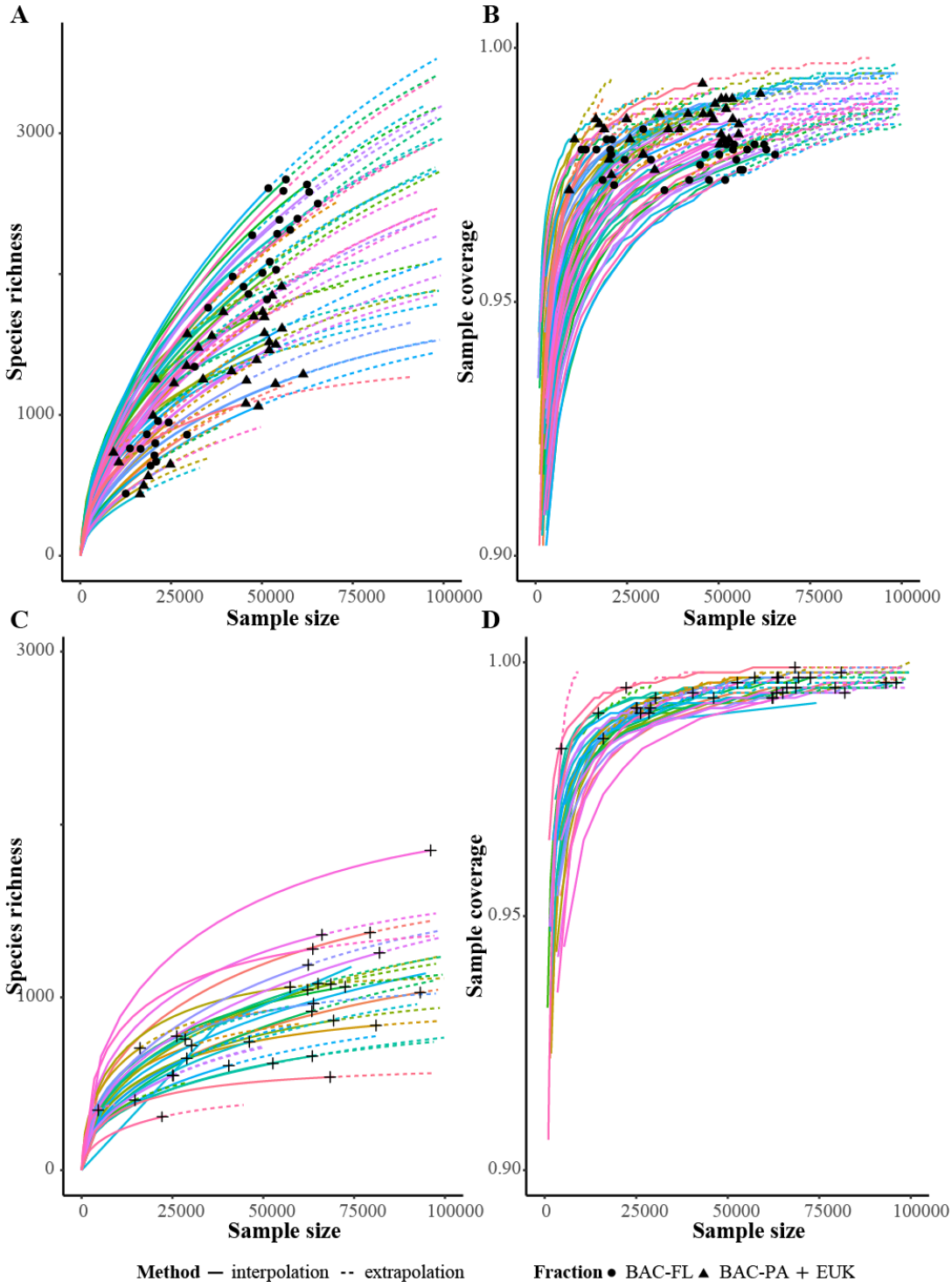

Supplementary Figure 2: Rarefaction analysis of bacterial and eukaryotic communities. (**A,C**) Sample-size-based rarefaction curves generated with the iNEXT package, for bacterial (A) and eukaryotic (C) communities. The solid lines represent the observed accumulation with the number of reads sampled, and the dashed lines represent the extrapolated accumulation up to the double amount of reads. Based on the Hill numbers of order q = 0. (**B,D**) Coverage-based sample completeness estimations for bacterial (B) and eukaryotic (D) communities. The observed values for each community are denoted by solid shapes.

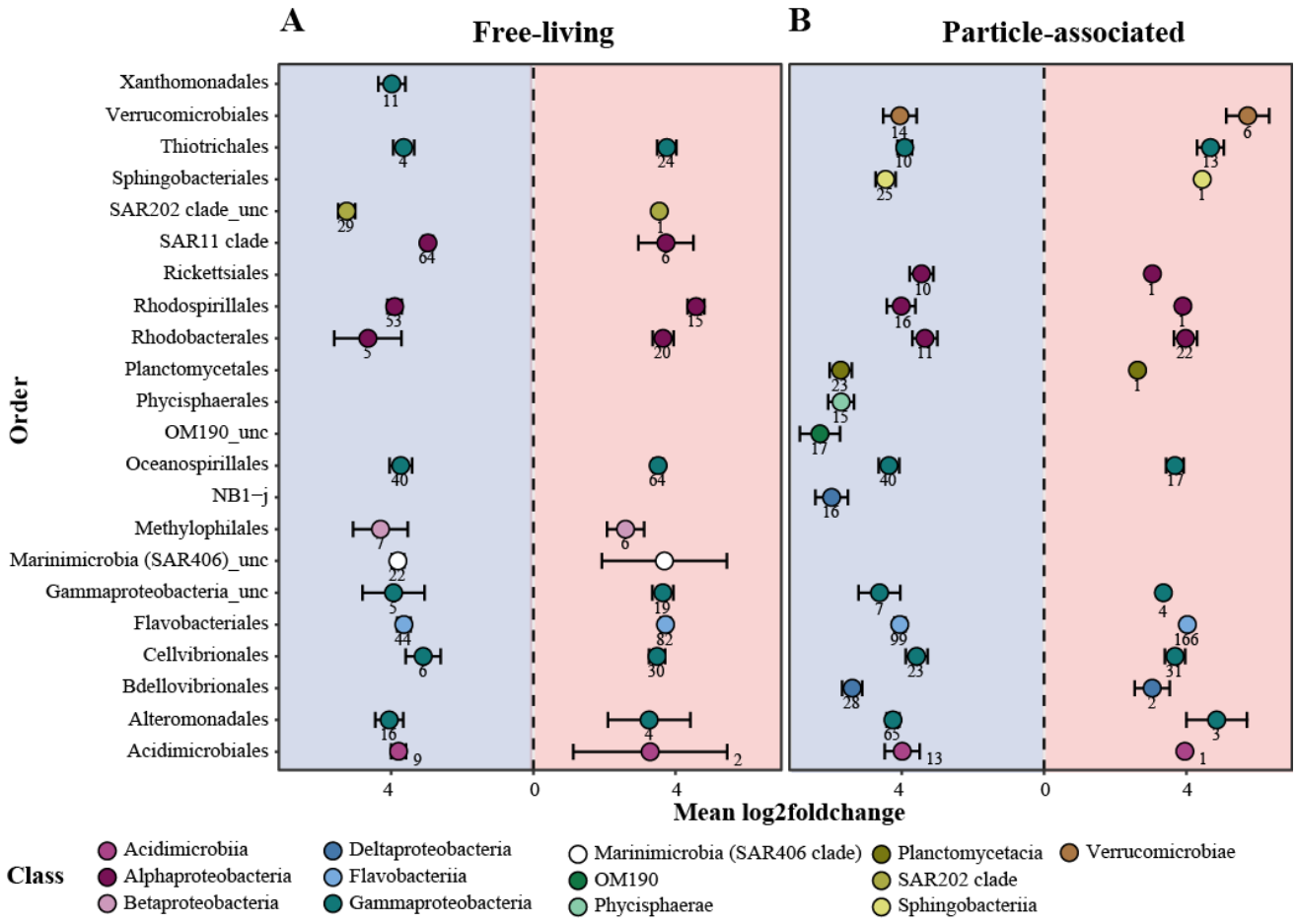

Supplementary Figure 3: Differences in bacterial community composition between the regions. OTU enrichment analysis was performed separately on the FL (**A**) and the PA (**B**) fractions, and only statistically significant daOTU were included in the data representation (adjusted p value < 0.05). The x axis represents absolute values of $\log_2$ fold change. Enrichment of daOTU in the EGC region is represented in the blue area, while enrichment in the WSC region is represented in the red area. The color code represents taxonomic classes and each point represents the average for orders with more than 10 daOTU (black bars indicate standard deviations). The numbers below the symbols represent the number of daOTU enriched in the region.

Supplementary Material

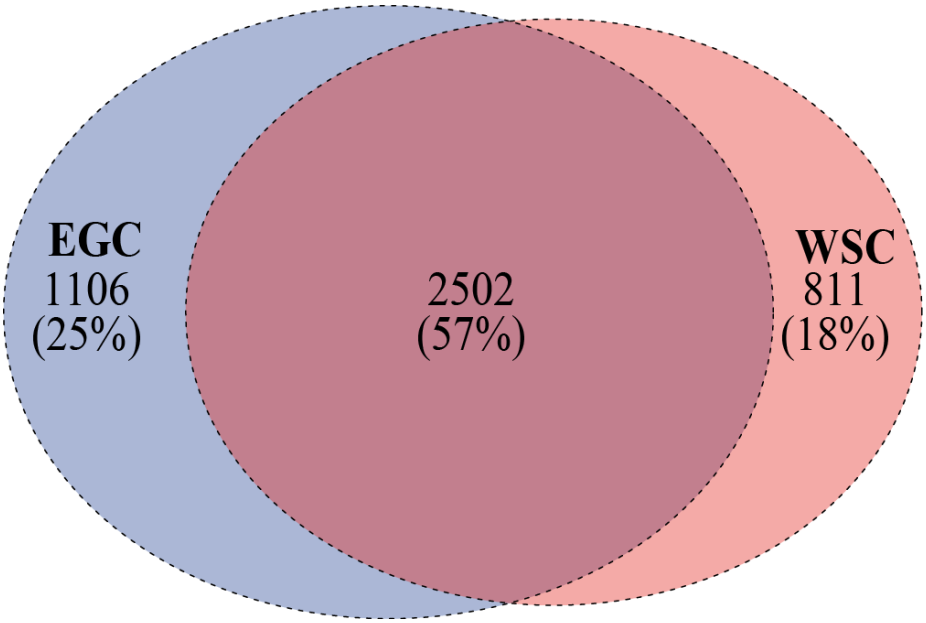

Supplementary Figure 4: Venn diagram of shared OTUs between microbial eukaryote communities in WSC and EGC.

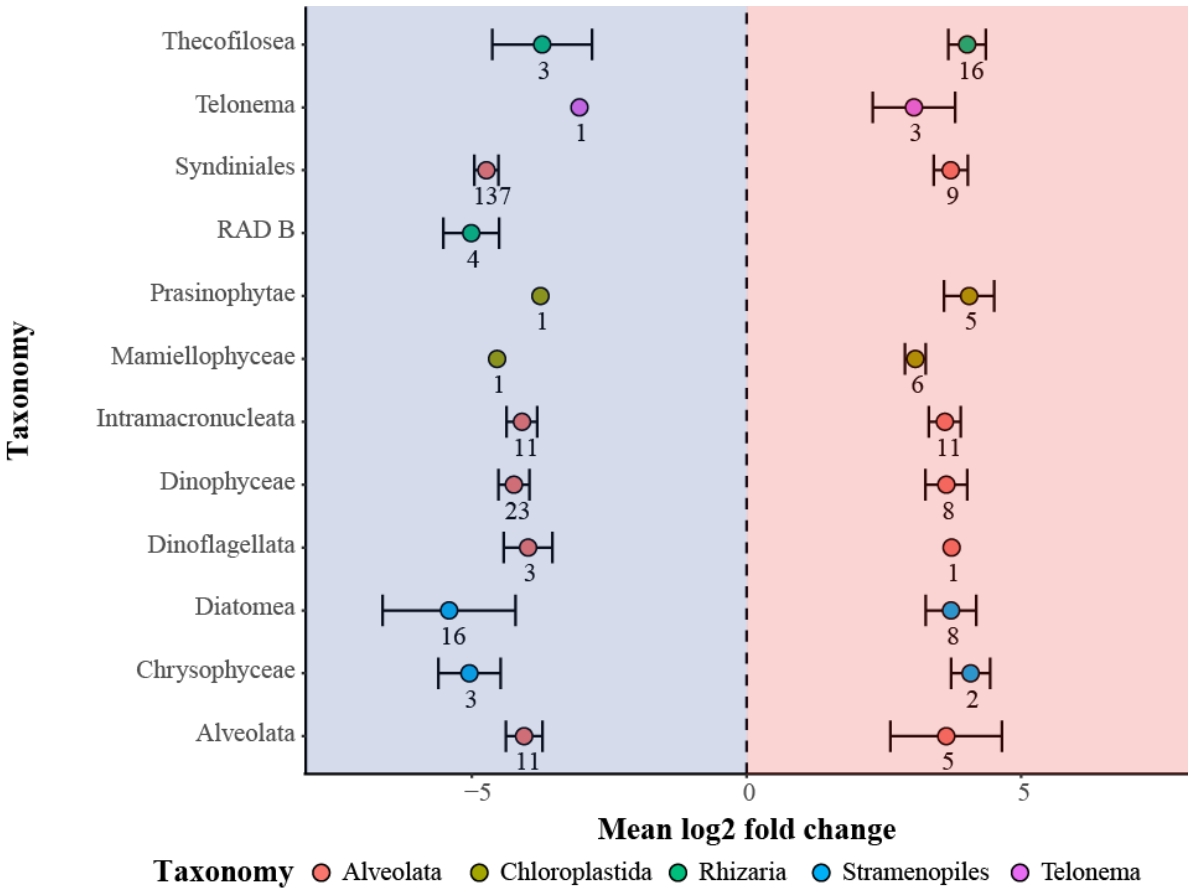

Supplementary Figure 5: Enriched microbial eukaryotic taxonomic groups between the regions. Only statistically significant taxa were included in data representation (p value < 0.05). The x axis represents the $\log_2$ fold change. Enrichment in EGC region is represented in the blue area while enrichment in the WSC region is represented in the red area. The color code represents higher taxonomic groups and each point represents the mean $\log_2$ fold change of all OTUs in the group (black bars indicate standard deviations).

Supplementary Material

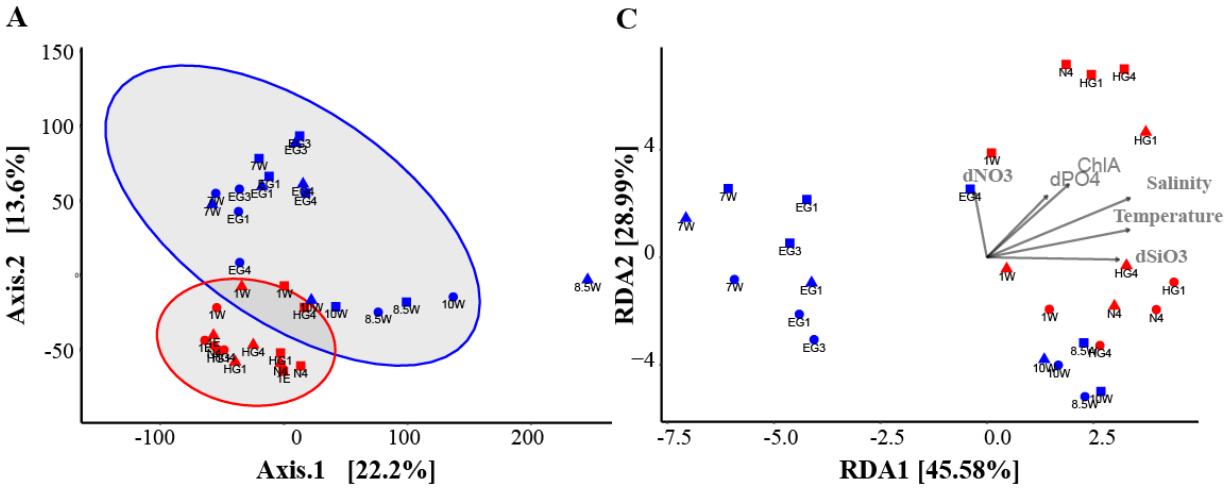

B

	F.model	R^2	p value
Region	4.5	0.13	0.001
Depth	1.28	0.07	0.120
Residuals		0.8	

Supplementary Figure 6: (**A**) PCoA of microbial eukaryote community composition in all three water layers. The ellipses encompass each of the groups with normal confidence of 0.95. The percentages on both axes represent the explained variance of the axis. (**B**) Permutational multivariate analysis of variance between samples ('ADONIS' in R package 'vegan'). (**C**) RDA ordination of eukaryote community composition constrained by environmental variables. The environmental variables are: Temperature, Salinity, ChlA - chlorophyll a, dSiO3 - ΔSiO3, dPO4 - ΔPO4 and dNO3 - ΔNO3.

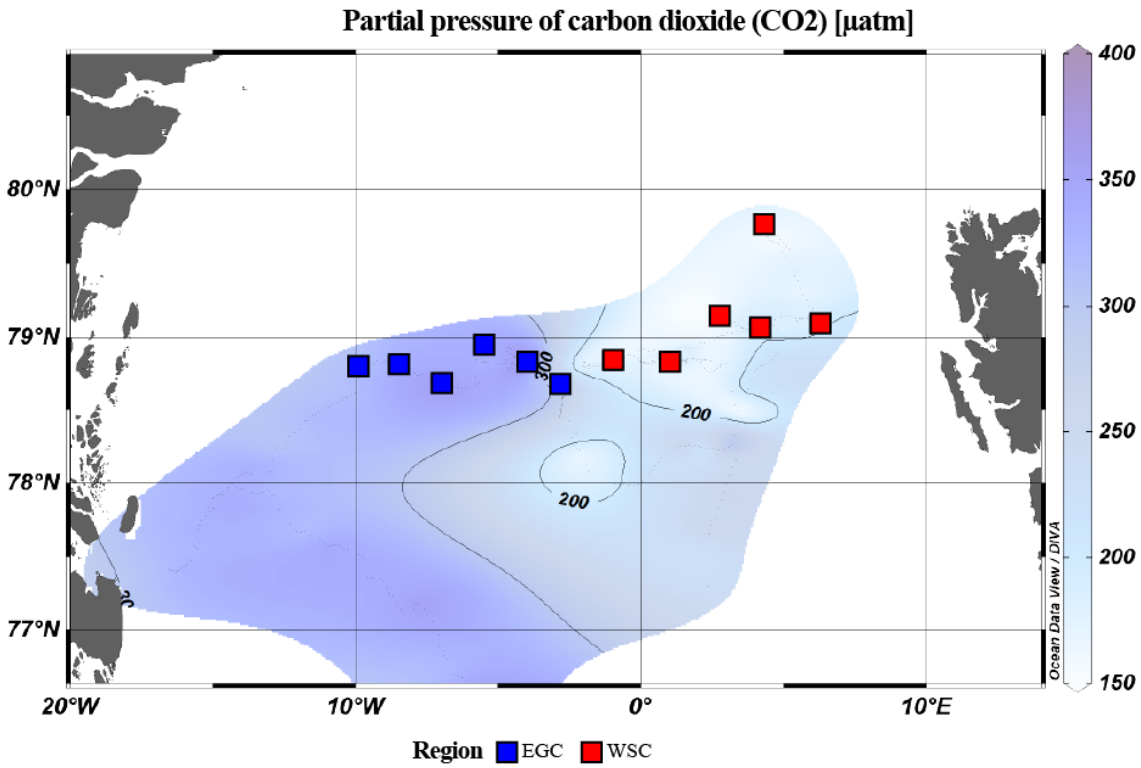

Supplementary Figure 7: Partial pressure of carbon dioxide (pCO_2) in surface waters across Fram Strait. The measurements were collected using an underway pCO_2 sensor mounted to the keel of the ship at 11 m depth (for further information: van Heuven and Hoppema, 2016).

Supplementary Material

2 Biogeochemical model FESOM-REcoM2

2.1 Description of the model

The biogeochemical model REcoM2 is a ratio model, in which stoichiometry is allowed to vary within set limits. The nutrients included in the model are nitrogen, silicon and iron, which describe the entire carbon cycle. The incoming photosynthetically available radiation (PAR) is prescribed by the JRA-55 reanalysis dataset (Kobayashi et al., 2015), and thus varies in time and space. The amount of PAR reaching the ocean surface at a given time and location is scaled to the ice concentration in each point of the surface grid. PAR decreases exponentially with depth and is further reduced by the presence of chlorophyll in the water. The growth rate of the model's two phytoplankton classes, nano-phytoplankton (e.g. flagellates) and diatoms is affected by light and nutrient availability. Degradation occurs through zooplankton grazing and bacterial activity, the latter of which is parameterized.

The biogeochemical tracers of REcoM2 are transported by ocean currents and mixing, which are provided by the ocean general circulation model FESOM (Wang et al., 2014). FESOM is characterized by a triangulated surface grid, making it possible to have increased resolution in selected areas. The current run is carried out in a global setup with a resolution of 4.5km north of 60°N (Wekerle et al., 2017). After spin-up of the ocean model, the coupled model was started in 1980 and run until 2015. The modeled biogeochemistry of 2010 to 2015 has been comprehensively described and assessed against available data, showing that the model describes well the Arctic marine biogeochemistry (Schourup-Kristensen et al., 2018). Moreover, in order to evaluate the modeled surface chlorophyll a trends, the modeled values in WSC (ice-free) were compared to remote sensing surface chlorophyll a measurements (Supplementary Figure 9). However, it is important to keep in mind that no model will perfectly catch the complexity of the biological systems; rather, the model results provide an insight into the biological processes and help us to look beyond the location and timing of *in situ* measurements.

2.2 Comparison of model output to satellite-based estimates of surface chlorophyll

To demonstrate the skill of the model we have plotted the monthly mean of surface chlorophyll *a* concentration from model output and from satellite-based estimates of chlorophyll (http://globcolor.com) for the year 2014 (Supplementary Figure 8). We compare to the satellite-based estimates as they provide a large-scale view of the development of the bloom in the area. Note that the satellite-based estimates use a specific algorithm for ocean color data (e.g. Maritorena et al., 2010). The satellite-based estimates should thus be regarded as another type of model. Agreement in the spatial and temporal distribution between the output from FESOM-REcoM2 and the satellite-based estimates indicates that they provide realistic results. For discussions of satellite-based estimates of productivity in the Arctic region, see e.g. Lee et al., 2016.

In FESOM-REcoM2, the bloom starts in the warm and nutrient-rich water of the Norwegian Atlantic Current in April and in the coastal waters of Iceland (Supplementary Figure 8A). This fits well with the satellite-based estimates (Supplementary Figure 8G). In May, the surface bloom covers the whole ice free area of the Nordic Seas in FESOM-REcoM2 (Supplementary Figure 8B). This is also the

case in the satellite-based estimates (Supplementary Figure 8H), but here the bloom is somewhat weaker compared to FESOM-REcoM2. The relatively strong bloom can be attributed to a low concentration of grazers early in the growth season, allowing the modeled bloom to develop to higher chlorophyll concentrations than in the ocean. From June onwards, the modeled chlorophyll *a* in the ice-free part of the Nordic Seas (Supplementary Figure 8C-F) has a very good fit with the satellite-based estimates (Supplementary Figure 8I-L). In the ice-covered region, the bloom begins as the ice concentration decreases in June, allowing PAR to reach the water column and initialize the bloom here (Supplementary Figure 8C).

To summarize, the productivity is at a post-bloom stage in the ice-free part of the Fram Strait in June for both FESOM-REcoM2 and satellite-based estimates. In the ice-covered part, the bloom begins during the month of June in the model results.

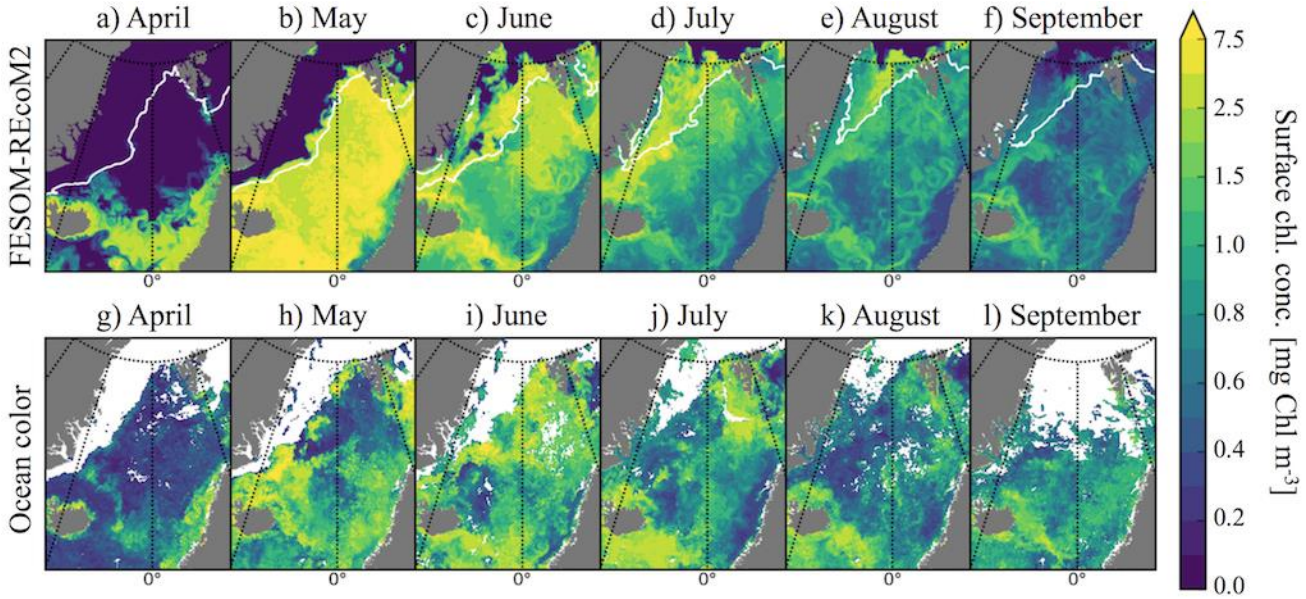

Supplementary Figure 8: Monthly mean of surface chlorophyll a in FESOM-REcoM2 (a-f) and in satellite-based estimates from Globcolor (g-l) downloaded from http://globcolor.com. Both model and satellite-based results are from 2014.The white line in subplot a-f marks the contour of the 10% ice concentration. White areas in subplots g-l are areas without data for the whole month, e.g. because of cloud cover or ice.

2.3 Comparison between modeled and in situ measured parameters in a section across the Fram Strait

For the cruise transect across the Fram Strait from Greenland to Svalbard at 78°N, we have plotted the vertical section of the mean June model results for temperature, salinity, chlorophyll and dissolved inorganic nitrogen (DIN). The model sections have been overlaid with the in situ measurements from the cruise (Supplementary Figure 9). The division between warm and salty Atlantic Water (AW) in the eastern Fram Strait and cold and fresher Arctic water in the western Fram Strait is clear in both the modeled results and the in situ measurements (Supplementary Figure 9A,B). In FESOM-REcoM2, the AW brings DIN to the Fram Strait from the south. In the surface layer, where PAR allows for productivity to take place, the DIN has been drawn down below concentrations that allow for phytoplankton growth, and consequently, productivity takes place deeper in the water column at the depth of the nitracline in the modeled eastern Fram Strait. This feature is a so-called chlorophyll maximum (chl a max, Supplementary Figure 9C,D). West of 5°E, where productivity starts later due to ice coverage, the nitracline is close enough to the surface that productivity can still take place in the uppermost part of the water column. In the in situ measurements, the nitracline is deeper in the eastern Fram Strait compared to FESOM-REcoM2, and the chl a max is thus also located deeper in the water column (Supplementary Figure 9C,D). The process behind the chl a max, namely the downwards movement of the nutricline due to biological uptake, is, however, the same in the model results and the in situ measurements, and indicates a later stage of the bloom in the eastern Fram Strait as compared to the western.

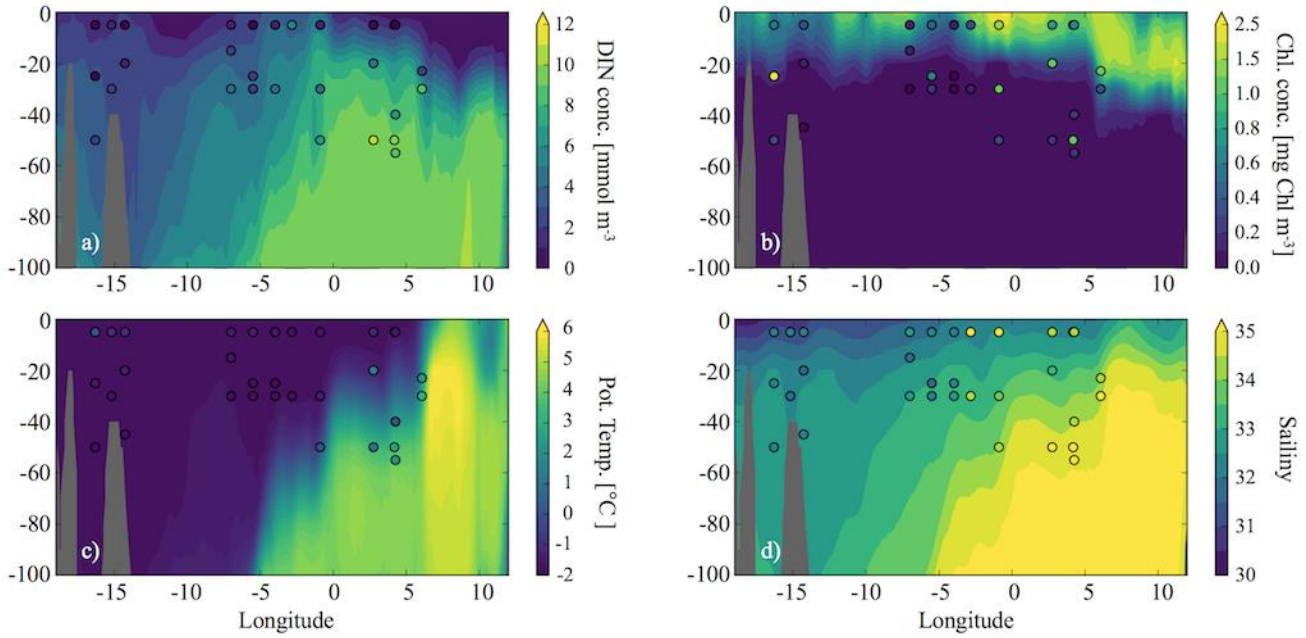

Supplementary Figure 9: Comparison of modeled and in situ measured parameters across the Fram Strait section at 78°N. The background represents the mean model results for June 2014, which have been overlaid with the in situ measurements from the PS85 expedition.

3 References

Kobayashi, S., Ota, Y., Harada, Y., Ebita, A., Moriya, M., Onoda, H., et al. (2015). The JRA-55 Reanalysis: General Specifications and Basic Characteristics. *J. Meteorol. Soc. Japan. Ser. II* 93, 5–48. doi:10.2151/jmsj.2015-001.

Lee, Y. J., Matrai, P. A., Friedrichs, M. A. M., Saba, V. S., Aumont, O., Babin, M., et al. (2016). Net primary productivity estimates and environmental variables in the Arctic Ocean: An assessment of coupled physical-biogeochemical models. *J. Geophys. Res. Ocean.* 121, 8635–8669. doi:10.1002/2016JC011993.

Maritorena, S., D'Andon, O. H. F., Mangin, A., and Siegel, D. A. (2010). Merged satellite ocean color data products using a bio-optical model: Characteristics, benefits and issues. *Remote Sens. Environ.* 114, 1791–1804. doi:10.1016/j.rse.2010.04.002.

van Heuven, S., and Hoppema, M. (2016). Underway physical oceanography and carbon dioxide measurements during POLARSTERN cruise PS85. *Bakker, Dorothee C E; Pfeil, Benjamin; O'Brien, Kevin M; Currie, Kim I; Jones, Stephen D; Landa, Camilla S; Lauvset, Siv K; Metzl, Nicolas; Munro, David R; Nakaoka, Shin-Ichiro; Olsen, Are; Pierrot, Denis; Saito, Shu; Smith, Karl; Sweeney, Colm; Tak. Taro; Wada, Chisato; Wanninkhof, Rik; Alin, Simone R; Becker, Meike; Bellerby, Richard G J; Borges, Alberto Vieira; Boutin, Jacqueline; Bozec, Yann; Burger, Eugene; Cai, Wei-Jun; Castle, Robert D; Cosca, Catherine E; DeGrandpre, Michael D; Donnelly, Matthew; Eischeid, Greg; Feel. Richard A; Gkritzalis, Thanos; González-Dávila, Melchor; Goyet, Catherine; Guillot, Antoine; Hardman-Mountford, Nicolas J; Hauck, Judith; Hoppema, Mario; Humphreys, Matthew P; Hunt, Christopher W; Ibánhez, J Sev. P; Ichikawa, Tadafumi; Ishii, Masao; Juranek, Lauren W; Kitidis, Vassilis; Körtzinger, Arne; Koffi, Urbain K; Kozyr, Alexander; Kuwata, Akira; Lefévre, Nathalie; Lo Monaco, Claire; Manke, Ansley; Marrec, Pierre; Mathis, Jeremy T; Millero, Frank J; Monacci, Natalie; Monteiro, Pedro M S; Murata, Akihiko; Newberger, Timothy; Nojiri, Yukihiro; Nonaka, Isao; Omar, Abdirahman M; Ono, Tsuneo; Padín, Xose Antonio; Rehder, Greg. Rutgersson, Anna; Sabine, Christopher L; Salisbury, Joe; Santana-Casiano, Juana Magdalena; Sasano, Daisuke; Schuster, Ute; Sieger, Rainer; Skjelvan, Ingunn; Steinhoff, Tobias; Sullivan, Kevin; Sutherland, Stewart C; Sutton, Adrienne; Tadokoro, Kazuaki; Telszewski, Maciej; Thomas, Helmuth; Tilbrook, Bronte; van Heuven, Steven; Vandemark, Doug; Wallace, Douglas WR; Woosley, Ryan Surf. Ocean CO2 Atlas V4. PANGAEA, https//doi.org/10.1594/PANGAEA.866856*. doi:10.1594/PANGAEA.865492.

Schlitzer, R. (2015). Ocean Data View. Available at: http://odv.awi.de.

Schourup-Kristensen, V., Wekerle, C., Wolf-Gladrow, D. A., and Völker, C. (2018). Arctic Ocean biogeochemistry in the high resolution FESOM 1.4-REcoM2 model. *Prog. Oceanogr.* 168, 65–81. doi:10.1016/j.pocean.2018.09.006.

Wang, Q., Danilov, S., Sidorenko, D., Timmermann, R., Wekerle, C., Wang, X., et al. (2014). The Finite Element Sea Ice-Ocean Model (FESOM) v.1.4: formulation of an ocean general circulation model. *Geosci. Model Dev.* 7, 663–693. doi:10.5194/gmd-7-663-2014.

Wekerle, C., Wang, Q., Danilov, S., Schourup-Kristensen, V., von Appen, W.-J., and Jung, T. (2017). Atlantic Water in the Nordic Seas: Locally eddy-permitting ocean simulation in a global setup. *J. Geophys. Res. Ocean.* 122, 914–940. doi:10.1002/2016JC012121.